Virtual multi-fracture craniofacial reconstruction using computer vision and graph matching

Ananda S. Chowdhury [a,*], Suchendra M. Bhandarkar [a], Robert W. Robinson [a], Jack C. Yu [b]

[a] Department of Computer Science, The University of Georgia, Athens, GA 30602, USA
[b] Department of Plastic Surgery, The Medical College of Georgia, Augusta, GA 30912, USA

ABSTRACT

The problem of computer vision-guided reconstruction of a fractured human mandible from a computed tomography (CT) image sequence exhibiting multiple broken fragments is addressed. The problem resembles 3D jigsaw puzzle assembly and hence is of general interest for a variety of applications dealing with automated reconstruction or assembly. The specific problem of automated multi-fracture craniofacial reconstruction is particularly challenging since the identification of opposable fracture surfaces followed by their pairwise registration needs to be performed expeditiously in order to minimize the operative trauma to the patient and also limit the operating costs. A polynomial time solution using graph matching is proposed. In the first phase of the proposed solution, the opposable fracture surfaces are identified using the Maximum Weight Graph Matching algorithm. The pairs of opposable fracture surfaces, identified in the first stage, are registered in the second phase using the Iterative Closest Point (ICP) algorithm. Correspondence for a given pair of fracture surfaces, needed for the Closest Set computation in the ICP algorithm, is established using the Maximum Cardinality Minimum Weight bipartite graph matching algorithm. The correctness of the reconstruction is constantly monitored by using constraints derived from a volumetric matching procedure guided by the computation of the Tanimoto Coefficient.

© 2009 Elsevier Ltd. All rights reserved.

1. Introduction

Craniofacial fractures are frequently encountered. The major causes are vehicle accidents, gunshot wounds and sports related injuries [1]. From a surgical perspective, craniofacial reconstruction becomes very complex in case of multiple fractures since the operating surgeon has to identify the opposable fracture surfaces before physically registering them. Often, the cost of surgery becomes prohibitive with the increased operative time necessary to complete the entire reconstruction process [2]. Moreover, the increased operative time also poses increased operative trauma and risk to the patient. The reconstruction problem essentially falls within the category of automated jigsaw puzzle solving and hence is of general interest in a variety of domains, ranging from forensics to archeology, that deal with problems related to automated reconstruction or assembly. As the mandible is often unprotected,

we concentrate specifically on mandibular fractures within the broad class of craniofacial fractures. In an earlier paper, we showed how computer vision algorithms can be applied to perform virtual reconstruction in case of a single fracture [3]. In this paper, we extend our earlier work to a multi-fracture scenario. The input to the current problem of automated craniofacial reconstruction is a computed tomography (CT) scan of a human mandible that exhibits multiple fractures. After performing simple image processing operations on the CT images, the broken bone fragments are separated from the soft tissue. The fracture surfaces in the broken fragments are highlighted manually by the surgeon. Thus, our reconstruction scheme is semi-automated as opposed to fully automated. A novel two step method based on graph matching is proposed as a solution to the multi-fracture registration problem. In the first step, the opposable fracture surfaces are identified using the Maximum Weight Graph Matching (MWGM) algorithm for a weighted graph. The fracture surfaces are modeled as vertices of a weighted graph. The edge weights in the graph are chosen as a linear combination of (a) the inverse Hausdorff distance and (b) an appropriately formulated function of curvature. In the second step, the opposable fracture surface pairs, identified in the first step, are registered using the Iterative Closest Point (ICP) algorithm. The surface point-wise correspondence between fracture surface pairs during each iteration of the ICP algorithm is determined using the

Maximum Cardinality Minimum Weight (MCMW) bipartite graph matching algorithm. The reconstruction process in the second step is constantly monitored by constraints derived from a volumetric matching procedure that is guided by the computation of the Tanimoto Coefficient. In [4] this work appeared in a preliminary version with no description of the image processing, limited details and only partial theoretical analysis.

The rest of the paper is organized as follows: Section 2 describes the existing literature and our contribution. Section 3 describes the image processing steps necessary to obtain the input data from the segmented fracture surfaces. Section 4 explains the formulation of the score matrix needed as an input to the MWGM algorithm. Section 5 proves the combinatorial nature of the problem (in terms of the number of reconstruction options) and illustrates how the MWGM algorithm identifies the opposable fracture surface pairs. Section 6 describes the pairwise fracture surface registration procedure using the ICP and MCMW algorithms. Section 7 explains the shape monitoring procedure based on the computation of the Tanimoto coefficient. Section 8 presents the experimental results. Section 9 concludes the paper and highlights directions for future research.

2. Literature review and our contribution

The multi-fracture reconstruction problem in a broader sense can be viewed as a combinatorial pattern matching problem that is similar to automated jigsaw puzzle solving (a detailed analysis is given in Section 5). We first discuss the importance of multiple mandibular and related craniofacial fractures in the surgical literature. Various existing approaches for solving two-dimensional (2D) and three-dimensional (3D) jigsaw puzzle problems are mentioned next. The section ends by highlighting the contribution of the paper.

In an article by Ogundare et al. [5], it is shown that 52% of the patients studied in a typical urban-level trauma center suffered from multiple mandibular fractures. In a study conducted by Boole et al. [6], about 30% of the army soldiers who experienced craniofacial trauma while on active duty suffer from two or more mandibular fractures. Clauser et al. [7] discuss the prevalence of severe midface fractures as a result of vehicular accidents, which could lead to surgical procedures involving high clinical complexity. It is interesting to note that in their work on multiple craniofacial injuries, Schettler et al. [8] suggest that the technique of surgical reconstruction in the case of craniofacial trauma is often tantamount to solving a jigsaw puzzle.

As the number of references in the research field of automated jigsaw puzzle solving is quite high, we restrict ourselves to discussing a few representative works. Research on jigsaw puzzle solving by means of a computer using images as input was initiated around 20 years ago with the work of Wolfson et al. [9]. In their seminal paper, they model the jigsaw puzzle solving problem as a Traveling Sales Person (TSP) problem. Webster et al. [10] identify critical isthmus points as robust global features for matching the pieces of a 2D jigsaw puzzle. The critical isthmus points are extracted using a medial axis transformation. Leitato and Stolfi [11] use multi-scale filtering, an initial matching followed by refinement and pruning of the search space with incremental dynamic programming to solve the 2D jigsaw puzzle problem. Goldberg et al. [12], on the other hand, address the same problem of 2D jigsaw puzzle reconstruction with a global relaxation approach after detection of fiducial points (robust canonical locations) on the 2D jigsaw puzzle pieces. Makridis and Papamarkos [13] propose a new technique which employs both geometrical and color features for jigsaw puzzle matching. Barequet and Sharir [14] present improved geometric hashing techniques for partial surface and volume matching in 3D for solving 3D jigsaw puzzles. Papaioannou et

al. [15] formulate a novel matching error metric for solving the 3D reconstruction problem via matching of individual parts using a 3D shape signature. Huang et al. [16] use integral invariants in the process of geometrically matching fragments of 3D objects. Some other important instances of the 3D jigsaw puzzle solving problem include the archaeological fragment assembly problem by Kampel and Sablantig [17]. The 3D earthenware assembly problem using axially symmetric shape descriptors for the broken fragments in conjunction with a Bayesian reconstruction procedure as formulated by Willis and Cooper [18] is also an instance of 3D jigsaw puzzle solving.

A flowchart of the proposed multi-fracture reconstruction scheme is diagrammed in Fig. 1. As shown in the figure, the reconstruction process is complete only after all the fracture surface pairs in a solution set s_i, derived from the MWGM algorithm, are registered satisfying the volumetric matching constraints. The primary contribution of the paper lies in proposing the MWGM algorithm for identification of opposable fracture surface pairs in CT image of a patient who has suffered severe craniofacial trauma. To the best of our knowledge, no work has so far been reported which uses a graph matching-based approach for virtual multi-fracture reconstruction in particular, and assembling a 3D jigsaw puzzle in general. A novel score matrix formulation which assists the graph matching algorithm in generating an optimal solution is presented. As mentioned earlier, the score matrix elements reflect the property of spatial proximity and the desirable surface characteristics between two opposable fracture surfaces. The second important contribution lies in the design of the
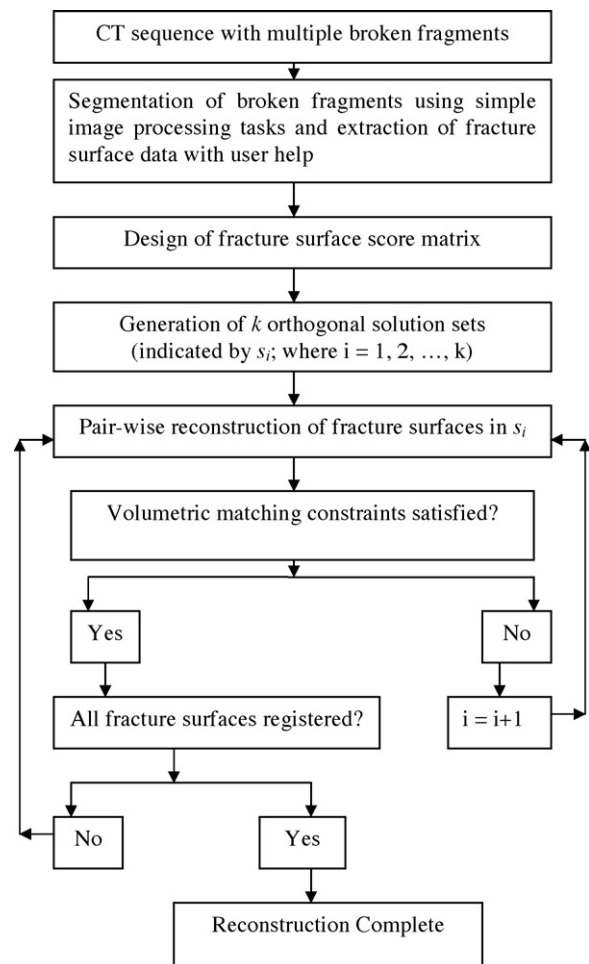

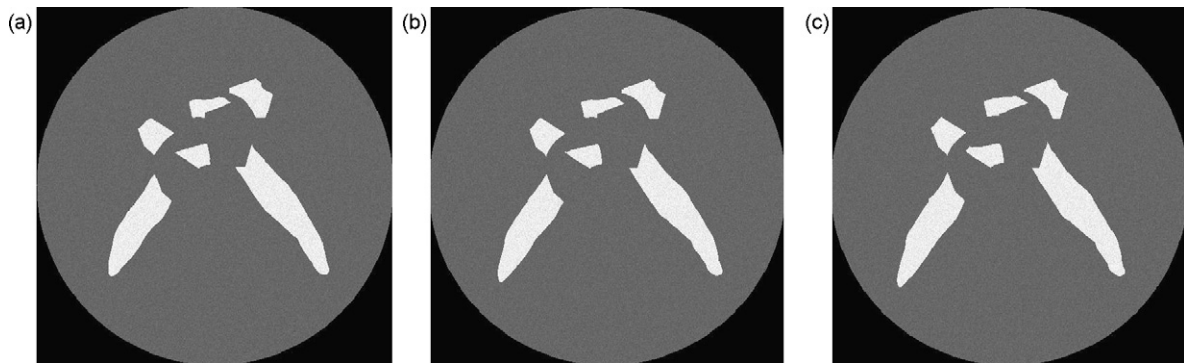**Fig. 1.** Flowchart for virtual multi-fracture reconstruction.

Fig. 2. A CT image sequence of a mandible with multiple fractures. The images in (a)–(c) represent three consecutive slices in the sequence.

MCMW algorithm for establishing a correspondence between two fracture surfaces while registering them using the ICP algorithm. Finally, monitoring the reconstruction process at each step using volumetric constraints also deserves special mention.

3. Image processing

The input to the computer vision-guided virtual craniofacial reconstruction procedure is a sequence of 2D grayscale CT images of a human mandible that exhibits multiple fractures. Fig. 2 shows three consecutive CT slices of such an image sequence. Some basic image processing procedures are undertaken to segment the broken bone fragments from the surrounding tissue. A surgeon then identifies the fracture surfaces and helps in extraction of the needed fracture surface data. A brief description of these tasks is given below.

In the CT images, the bright area with higher Hounsfield unit values [19] represent the fractured mandible (bone) fragments whereas the dark areas with relatively lower Hounsfield unit values represent the surrounding soft tissue. Hence, the threshold value for the binarization of the CT image is not difficult to select and simple thresholding was observed to be sufficient. For a grayscale CT image slice $G(i, j)$, we obtain a binary image $B(i, j)$ by setting

$$B(i,j) = \begin{cases} 1 & \text{if } G(i,j) > T, \\ 0 & \text{otherwise} \end{cases} \tag{1}$$

The result of the simple thresholding is shown in Fig. 3, where the broken fragments are represented by the highest intensity value and everything else by the lowest intensity value. A 2D Connected Component Labeling (CCL) procedure is used on the binary image. The results of the 2D CCL procedure are propagated across the CT image slices, resulting in a 3D CCL algorithm. A 3D component (a fractured jaw bone in this case) is identified by computing the area of overlap of the corresponding 2D components in successive CT image slices.

The result of the CCL procedure is shown in Fig. 4, where the six broken fragments are represented by six different grayscale values and the background pixels are assigned the highest intensity value for better visualization. The fracture surfaces on the broken bone fragments are identified manually by the surgeon in the current implementation. The task of interactive contour data extraction is performed on each of the binary image slices. A surgeon/user is required to click on the end points of the fracture contours in each of the binary image slices. The intervening contour points are then automatically generated using a contour tracing algorithm. The contour points, obtained from the individual binary image slices, are collated to generate the 3D surface point dataset. A 3D surface point dataset is thus generated for each fracture surface. The above image processing tasks are necessary to obtain the surface data for all the fracture surfaces corresponding to the broken bone fragments. The fracture surface data is used as input for solving the combinatorial pattern matching problem and generating the 3D transformation for surface registration. The 3D transformation is then applied to the appropriate bone fragments for the purpose of virtual reconstruction.

4. Design of a score matrix

A score matrix is formulated based on the appearance of various mandibular fragments in the input CT image sequence. The mandibular fragments are classified as *terminal* or *non-terminal*, based on the presence or absence of condyles (an extremity of the human mandible that exhibits pronounced sphericity), respectively. It is worth-mentioning that this type of prior rudimentary classification of the bone fragments to be assembled is similar to the schemes of Wolfson *et al.* [9] and Goldberg *et al.* [12] in the context of automated jigsaw puzzle solving. Both Wolfson *et al.* and Goldberg *et al.* separately assemble the *border* and *interior* frame pieces of a jigsaw puzzle. In fact, Goldberg *et al.* further classify
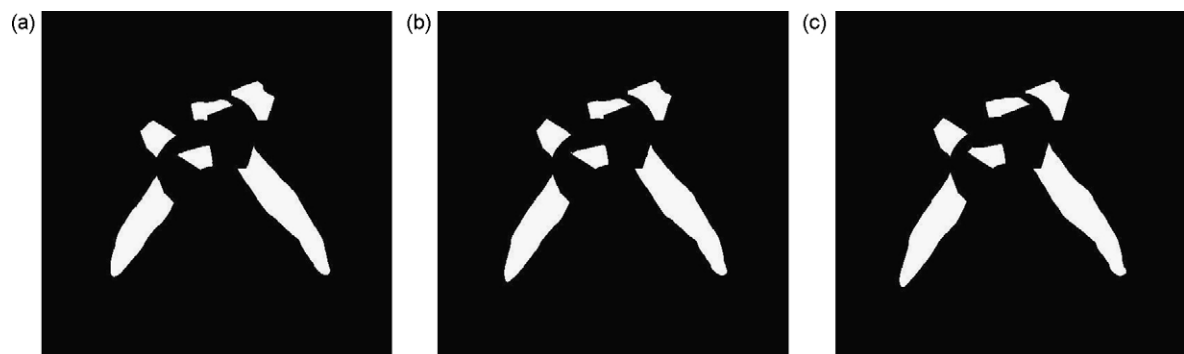

Fig. 3. The result of thresholding on the three CT slices in Fig. 2. The broken fragments are shown in white while the background is shown in black.
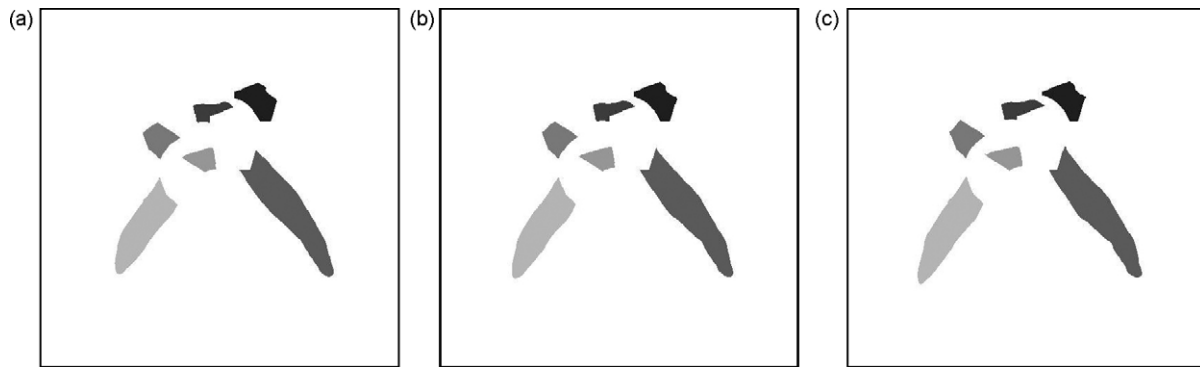
(a) (b) (c)

Fig. 4. The result of connected component labeling on the three CT slices in Fig. 2. Each broken fragment is represented by a separate grayscale value.

the border pieces as indents, outdents and flat sides. A terminal fragment in our case is similar to a border piece of a jigsaw puzzle whereas a non-terminal fragment corresponds to an interior piece of a jigsaw puzzle. A terminal fragment is often found to contain a single fracture surface. By contrast, a non-terminal fragment often exhibits two fracture surfaces (for example, please see Fig. 5). In the present work, experiments and subsequent mathematical analysis are based on the assumption that a terminal fragment has one fracture surface and a non-terminal fragment has two fracture surfaces. However, the proposed scheme is flexible enough to handle any number of fracture surfaces for a given fragment. Each fracture surface is represented by a collection of 3D data points obtained by extracting and collating the corresponding fracture contour points in the individual 2D CT image slices. In the case of 2D jigsaw puzzle solving, the score matrix formulation is based typically on curve matching, where the matrix elements denote the compatibility between potentially opposable edge points [20,21]. In our case, we need to estimate the matching score between the 3D fracture sur-

faces extracted from the CT image slices. A high matching score is assigned to a pair of fracture surfaces if (a) they are determined to be spatially proximal, and (b) they are determined to exhibit complementary (opposable) fracture surface characteristics. We have used both of these factors in determining the matching score for the proposed score matrix formulation.

4.1. Mathematical formulation of spatial proximity

The various fracture surfaces under consideration possess a varying number of data points. The formulation of a distance measure (*i.e.*, a measure of spatial separation) between any surface pair requires the establishment of correspondence between the data points on the two surfaces. Given the dimensions of the score matrix, *i.e.*, the number of possible fracture surface pairs for which the above correspondence has to be established beforehand, the task of determining a distance measure is computationally very expensive. We therefore use the Hausdorff distance, which does not need prior determination of correspondence between the two data point sets, to yield a measure of spatial separation between them. The Hausdorff distance H(A, B) between two datasets A and B is given [22] by:

$$H(A, B) = \max(h(A, B), h(B, A)),\tag{2}$$

where $h(A, B)$ denotes the *directed* Hausdorff distance between the two datasets A and B and is defined as

$$h(A, B) = \max_{a \in A}(\min_{b \in B}\|a - b\|).\tag{3}$$

Here $\|a - b\|$ represents the Euclidean distance between the points a and b. Each such a, and b, in our case, is a 3D data point in the fracture surface data set A and B, respectively. The computation of the Hausdorff distance can be performed directly in $O(mn)$ time, *i.e.*, quadratic polynomial time, where m and n denote the cardinalities of the two fracture surface data sets under consideration.

4.2. Mathematical formulation of surface characteristics

There are well-known measures for characterizing 3D surfaces described in the computer vision literature, of which the *Gaussian* and *Mean* curvatures are the most prominent [23]. Each fracture surface in the present scenario is viewed as a collection of several fracture contours. It is to be noted that the determination of the Gaussian and Mean curvatures is relatively computationally intensive and also more sensitive to noise as compared to the determination of contour curvature. The choice of contour curvature as a measure of surface irregularity is further justified by the fact that it also possesses the properties of rotational and translational invariance [24]. The *contour curvature* for a point (x, y) in a given CT image

Non-terminal Fragments with fracture surfaces numbered as {4, 5}, {2, 3}, {6, 7} and {8, 9}

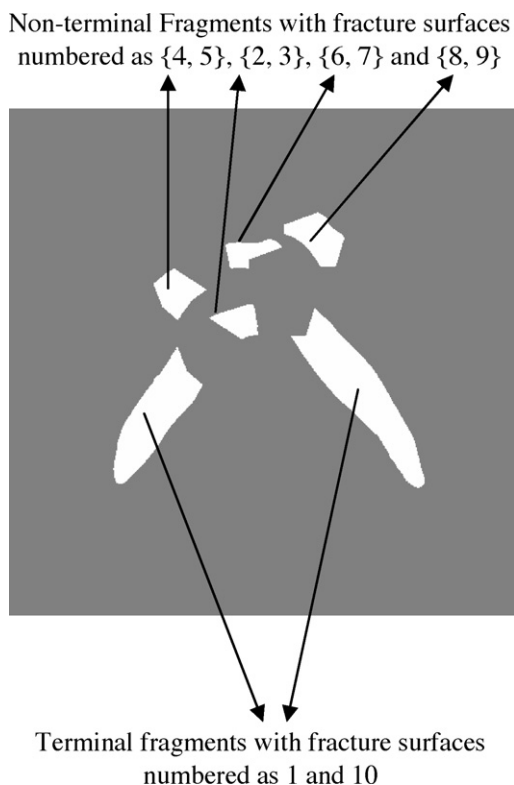Terminal fragments with fracture surfaces numbered as 1 and 10

Fig. 5. A Single 2D slice showing the terminal and non-terminal fragments with the fractured contours.

slice (for a specific value of z) is given by [24]:

$$c(x, y) = \frac{(d^2y/dx^2)}{\left(1 + (dy/dx)^2\right)^{3/2}}. \tag{4}$$

We formulate a function which captures the compatibility between two fracture surfaces using contour curvature. The function $FS(A, B)$ for a pair of surfaces A, B is defined as the sum of the scores $fs(a, b)$ for each possible point pair, one point from each of the surfaces. If the two points under consideration have the same signs for their contour curvatures, then they cause the overall surface matching score to increase; otherwise they cause it to decrease. Thus, we can write:

$$FS(A, B) = \sum_{a \in A} \sum_{b \in B} fs(a, b). \tag{5}$$

Intuitively, the score $fs(a, b)$, between any pair of points a, and b, is high if (a) the slice-wise locations of two points are spatially proximal, and (b) the relative positions of the two points in their respective slices (estimated using the end-points of the slices as the reference points) are proximal and (c) the curvature values of the two points are close. The score will be low if any of the above criteria is not satisfied. Thus, we can quantitatively express $fs(a, b)$ as the product of the above three factors and a sign function:

$$fs(a, b) = S(a, b)E(a, b)C(a, b)sg(c_a c_b) \tag{6}$$

where

$$
\begin{aligned}
S(a, b) &= \frac{2}{1 + \exp(|s_a - s_b|)}, \\
E(a, b) &= \frac{2}{1 + \exp(|e_a - e_b|)}, \\
C(a, b) &= \frac{2}{1 + \exp(|c_a - c_b|)}, \\
sg(c_a c_b) &= \begin{cases} +1 & \text{if } c_a c_b > 0 \\ -1 & \text{if } c_a c_b < 0. \end{cases}
\end{aligned}
\tag{7}
$$

Here $S(a, b)$, $E(a, b)$ and $C(a, b)$ respectively denote the slice-wise location-based score, relative position within the slice-based score and the curvature value-based score of the two surface points a and b where $s_a(s_b)$, $e_a(e_b)$, $c_a(c_b)$ respectively denote the slice value, relative position value of the surface point within the slice and contour curvature value (given by Eq. (4)) of the surface point $a(b)$.

4.3. Elements of the score matrix

The elements of the score matrix $SC(A, B)$ are computed as a linear combination of the inverse Hausdorff distance and the surface matching score:

$$SC(A, B) = \lambda_1 H^{-1}(A, B) + \lambda_2 FS(A, B) \tag{8}$$

where the coefficients of the linear combination are determined using the following constraints:

$$
\begin{aligned}
\lambda_1 + \lambda_2 &= 1, \\
\frac{\lambda_1}{\sigma(H^{-1}(A, B))} &= \frac{\lambda_2}{\sigma(FS(A, B))}.
\end{aligned}
\tag{9}
$$

In Eq. (9), $\sigma(H^{-1}(A, B))$ and $\sigma(FS(A, B))$, respectively, denote the standard deviation of the terms $H^{-1}(A, B)$ and $FS(A, B)$ for all possible fracture surface pairs A and B. Let us denote the number of fracture surfaces by nfs and enumerate the fracture surfaces as $1, 2, \ldots, nfs$.

5. Identification of opposable fracture surfaces

In this section, we first derive an expression showing the exponential behavior of the current reconstruction problem in terms of number of reconstruction options. Next, using a Maximum Weight Graph Matching algorithm, we show how we can identify the juxtaposable fracture surface pairs in polynomial time.

5.1. Combinatorial nature of the reconstruction problem

Theorem 1. *Given that a non-terminal fragment has two fracture surfaces and a terminal fragment has one fracture surface, the number of possible reconstruction options rc_n, where n is the total number of fragments, is given by*: $rc_n = (n-2)!2^{(n-2)}$.

Proof. With n fragments in total, we have $(n-2)$ non-terminal fragments and 2 terminal fragments. The $(n-2)$ non-terminal fragments can be encountered in any of $(n-2)!$ possible orderings. Furthermore, each non-terminal fragment can be oriented such that either of the fracture surfaces is the first surface in the sequence. This accounts for the factor $2^{(n-2)}$ in counting the number of possibilities. □

The presence of a factorial and an exponential term in the above expression for rc_n clearly demonstrates the combinatorial nature of the reconstruction problem in terms of the number of reconstruction options. Thus, an exhaustive search to identify the opposable fracture surfaces quickly becomes impractical. Note that even for such a reasonably small number of fragments as 6, the number of reconstruction options is already 384. It is important to mention that the analysis with the assumption of two fracture surfaces *per* non-terminal fragment and one fracture surface *per* terminal fragment can be easily generalized when the above assumptions are relaxed.

5.2. Maximum weight graph matching for restricting the reconstruction options

As mentioned in the literature review, various algorithmic and computational geometry-based approaches have been undertaken to restrict the number of reconstruction options for the jigsaw puzzle problem. We use the *Maximum Weight Graph Matching* algorithm to achieve this goal by generating k solution sets, where $k \geq 2$ and the solution sets are indexed by $j, j = (1, \ldots, k)$. A result on the time complexity of MWGM algorithm is stated (without proof) below.

Theorem 2. *The worst-case time complexity of the maximum weight graph matching (MWGM) algorithm for a graph $G = (V, E)$ with $|V| = n$ is $O(n^4)$.*

For a detailed proof of the above theorem we refer the interested reader to [25,26]. We state and justify the following claim regarding the modeling of the current reconstruction problem as a MWGM problem.

Claim 1. *The Maximum Weight Graph Matching algorithm for a weighted graph correctly identifies a number of solution sets, where each individual solution set is guaranteed to include all the fracture surfaces given by a collection of unordered opposable fracture surface pairs, in polynomial time.*

Justification: The fracture surfaces are modeled as the vertices of a weighted graph $G = (V, E)$. Let w_{AB} be the weight of an edge between two vertices (fracture surfaces in this problem) A and B (where A, B belongs to V). The anatomical constraints preclude placement of edges between certain pairs of vertices. For these edges, we set $w_{AB} = 0$. For other edges, we assign the pre-computed

real symmetric score matrix elements $SC(A, B)$ (from Eq. (8)) to w_{AB}. The goal is to identify the sets of opposable fracture surfaces such that the sum of the matching scores is maximized. Thus, the current reconstruction problem maps to the following well-known maximum weight graph matching problem in graph-theory, i.e., given a weighted undirected graph $G = (V, E)$ with edge weights $w_{AB} \geq 0$, obtain a pairing of the vertices such that the sum of the edge weights $\sum w_{AB}$ is maximized. The number of vertices of our graph is even and hence a complete/perfect matching is guaranteed, i.e., a solution set will always include a possible pairing of all the (opposable) fracture surfaces. Furthermore, since the score matrix is symmetrical and the graph is undirected, the ordering within an individual pair of surfaces does not matter. Once a solution is generated, the edge weights for all pairs in it are set to 0 prior to generating the next solution. Thus successive solutions are disjoint sets of pairs (of fracture surfaces). Each successive solution obtained by the MWGM algorithm set will lead to a decrease in the value of $\sum w_{AB}$ compared to its previous solution. Let the sum of edge-weights in two successive solutions (j and ($j + 1$)) be denoted by $\sum w_{AB}^{j}$ and $\sum w_{AB}^{j+1}$, respectively. We continue to generate k solution sets from the MWGM algorithm unless the following constraint is violated:

$$\left(\sum w_{AB}^{j} - \sum w_{AB}^{j+1}\right) < p \sum w_{AB}^{j}. \tag{10}$$

where p is an appropriately chosen positive constant (0.1 for the present problem). From Theorem 2, the MWGM algorithm for a weighted graph G with n vertices (i.e., $n = |V|$), has $O(n^4)$ run-time complexity. If we generate k orthogonal solution sets with no edges in common (according to Eq. (10)), where k is usually much less than n, then the time-complexity of our proposed solution is $O(kn^4)$, which is polynomial.

6. Pairwise registration of the fracture surfaces

The fracture surface pairs are first registered using the ICP algorithm described in [28] with the incorporation of a novel graph-theoretic enhancement. The main steps in the enhanced ICP algorithm [4] are as follows:

(1) The matching points in one fracture surface data set, called the *model data set*, that correspond to points in the other fracture surface data set, called the *sample data set*, are determined and termed as the *closest set*. The matching point pairs are determined using the MCMW bipartite graph matching algorithm [26]. The use of the MCMW bipartite graph matching algorithm obviates the need for any prior alignment of the two fracture surface data sets when computing the *closest set* in the ICP algorithm.

(2) The 3D rigid body transformation computed using the closest set is applied to the original sample data set and the Mean Squared Error (MSE) between the transformed sample data points and the corresponding closest points is computed. The MSE (ϵ^2) is given by

$$\epsilon^2 = \left(\frac{1}{p}\right) \sum_{i=1}^{p} ((c_i - (Rs_i + T))^2) \tag{11}$$

where R denotes the rotation matrix, T denotes the translation vector, s_i denotes a point in the sample data set, c_i represents the corresponding point in the closest set and $p = \min\{|V_1|, |V_2|\}$ (where $|V_1|$ and $|V_2|$ denote the cardinalities of the two fracture surface datasets).

The above two steps are repeated with an updated sample set (generated by applying R and T obtained in the current iteration

to the current sample set) until a pre-specified error convergence criterion (0.01 in our case) is reached. Next, we elaborate upon the MCMW bipartite graph matching algorithm and justify an associated claim.

Theorem 3. *The worst-case time-complexity of the Maximum Cardinality Minimum Weight (MCMW) matching algorithm for a bipartite graph $G = (V_1 \cup V_2, E)$ with $|V_1| = |V_2| = n$ is $O(n^3)$.*

For the proof of the above theorem we refer the interested reader to [25,26].

Claim 2. *Given that in typical cases of craniofacial injury, the rotational or translational displacements are not very large, the Maximum Cardinality Minimum Weight (MCMW) matching algorithm for a bipartite graph correctly establishes the correspondence between two fracture surfaces at every stage of the Iterative Closest Point (ICP) algorithm in polynomial time.*

Justification: Our justification is based on Theorem 3. Each fracture surface, consisting of several 3D data points, is modeled as a vertex set of a weighted bipartite graph $G = (V_1 \cup V_2, E)$. The bipartite graph is complete, i.e., there exists an edge $e_{ij} \in E$ between each vertex pair (v_i, v_j) where $v_i \in V_1$ and $v_j \in V_2$. The weight w_{ij} of edge e_{ij} is chosen to be the Euclidean distance between the corresponding vertices $v_i \in V_1$ and $v_j \in V_2$ where $i = 1, 2, \ldots, n_1, j = 1, 2, \ldots, n_2$, $n_1 = |V_1|$ and $n_2 = |V_2|$. The vertex set with lower cardinality is termed the *sample set* and that with the higher cardinality is termed the *model set*. The goal is to compute the *closest set*, i.e., a maximal subset of the model set wherein each point corresponds to a unique point in the sample set such that all points in the sample set are exhausted (principle of maximum cardinality) and simultaneously the sum of the edge weights between all pairs of corresponding points (i.e., $\sum w_{ij}$) is minimized (principle of minimum weight). This procedure is performed in each iteration of the ICP algorithm. In case of small or moderate translational or rotational displacements of the broken bone fragments, typical for a craniofacial injury, this graph theoretic optimization procedure, with an objective function that is formulated as the *sum of the Euclidean distances between all the pairs of matched points*, correctly matches a sample point with a model point without distorting the shape of the fracture surfaces. A greedy approach [27], based on the minimum Euclidean distance between individual pairs of points considered one at a time, on the other hand, would map more than one sample point to a single model point and distort the fracture surface shape. Our problem formulation maps to the following well-known Maximum Cardinality Minimum Weight (MCMW) Bipartite Graph Matching Problem in graph theory, i.e., given a weighted complete bipartite graph $G = (V_1 \cup V_2, E)$ with edge-weights $w_{ij} \geq 0$, determine a pairing of the vertices between sets V_1 and V_2 such that the vertex set with smaller cardinality is completely exhausted and the total cost of the pairings is minimum. By virtue of its construction the proposed bipartite graph is complete with $E = V_1 \times V_2$ where $|V_1| \leq |V_2|$, so a maximum cardinality matching must contain n_1 edges. From Theorem 3, the MCMW algorithm runs in $O(n^3)$ time for a bipartite graph with two vertex sets of equal cardinality n. In our case we take $n = max(n_1, n_2)$. Thus, the proposed solution clearly runs in polynomial time.

7. Shape monitoring of the reconstructed mandible

Note that we have so far used (a) a score matrix that is formulated in a manner that is favorable to an optimal solution and (b) a non-greedy MWGM algorithm to solve the problem of multifracture reconstruction. In this section, we exploit the knowledge of the global shape of a human mandible to monitor and verify the reconstruction process at each step. The literature on automated jigsaw puzzle assembly includes such a verification or validation

procedure. For example, Burdea and Wolfson [29] discuss robotic verification of a jigsaw puzzle assembly following the machine vision and the combinatorial optimization algorithms. Our overall strategy in solving the multi-fracture reconstruction problem is along similar lines. Using the MWGM algorithm in the manner described in Section 5.2, we can generate multiple solution sets where each solution set is a collection of fracture surface pairs. The overall approach is to start with the best solution set and perform shape checking after every additional fracture surface pair is registered. At any stage in the reconstruction procedure if the shape matching constraint(s) is(are) violated, we abandon the current solution and restart the registration procedure with the next best amongst the orthogonal solutions produced by the MWGM algorithm. Since the desired outcome of the reconstruction is known *a priori*, we can actually use the desired outcome or a close approximation thereof as a reference. We use an unbroken human jaw as a reference shape for this purpose. We compare the partially reconstructed jaw at every stage of the reconstruction procedure with the unbroken reference jaw. There are several shape matching algorithms described in the computer vision literature [30,31]. We employ two constraints based on the Tanimoto coefficient [32] in the context of volumetric shape matching. The Tanimoto coefficient $TC_{f,g}$ between two volumetric shapes f and g is defined as follows [32]:

$$TC_{f,g} = \frac{O_{f,g}}{I_f + I_g - O_{f,g}} \quad (12)$$

where

$$I_f = \int \int \int f^2(\hat{x}, \hat{y}, \hat{z}) dx dy dz \quad (13)$$

$$I_g = \int \int \int g^2(\tilde{x}, \tilde{y}, \tilde{z}) dx dy dz \quad (14)$$

$$O_{f,g} = 2 \int \int \int f(\hat{x}, \hat{y}, \hat{z}) g(\tilde{x}, \tilde{y}, \tilde{z}) dx dy dz \quad (15)$$

Here $(\hat{x}, \hat{y}, \hat{z}) = (x - x_{RC}, y - y_{RC}, z - z_{RC})$ and $(\tilde{x}, \tilde{y}, \tilde{z}) = (x - x_{SC}, y - y_{SC}, z - z_{SC})$ respectively represent the points of the reference mandible R and the reconstructed mandible S with respect to their individual centroids denoted by (x_{RC}, y_{RC}, z_{RC}) and (x_{SC}, y_{SC}, z_{SC}). Here f and g denote the characteristic functions of R and S, *i.e.*,

$$f(\hat{x}, \hat{y}, \hat{z}) = \begin{cases} 1 & \text{if}(\hat{x}, \hat{y}, \hat{z}) \in R \\ 0 & \text{otherwise} \end{cases} \quad (16)$$

$$g(\tilde{x}, \tilde{y}, \tilde{z}) = \begin{cases} 1 & \text{if}(\tilde{x}, \tilde{y}, \tilde{z}) \in S \\ 0 & \text{otherwise} \end{cases} \quad (17)$$

Now, we state and justify the following claim about the constraints based on volumetric matching derived from the Eqs. (12)–(17).

Claim 3. *The following two shape constraints based on volumetric matching are sufficient to determine the correctness of the reconstruction procedure at any stage*:

(a) $TC_{f,g}$ *is monotonically non-decreasing.*
(b) $2I_g - O_{f,g} \leq 2qI_g$ *where q is a small positive number (chosen as 0.01 for the present problem).*

Justification: At each stage of the reconstruction procedure, an additional bone fragment is added to the partially reconstructed mandible thus far. Ideally (if S is contained in R) then adding a fragment to S increases the numerator in the defining Eq. (12) and decreases the denominator. So, if $TC_{f,g}$ decreases when a fragment is added that's compelling evidence that the

Table 1
Extreme score parameter values.

Score parameter extremes	Value	Fracture surface pair
Min. overall score	1	(4, 9)
Max. overall score	1362	(1, 4)

solution set we are working with is wrong and should be abandoned. This justifies the constraint (a). Note that the reference mandible remains the same throughout the reconstruction procedure, whereas the reconstructed mandible increases in volume in successive stages of reconstruction. Furthermore, note that both, the reference mandible and the reconstructed mandible under consideration, are binary objects. It is quite evident from the Eqs. (12)–(17) that at any stage, the extent of the volumetric overlap O_{fg} should be exactly twice the reconstructed volume I_g, but again only in the ideal case. So, for a satisfactory solution set, we expect that the inequality should hold for a small value of q (chosen as 0.01 for the present problem). Thus, we obtain $1 - O_{fg}/2I_g < q$. Multiplying both sides by $2I_g$, we get the desired result (b).

8. Analysis of experimental results

The crux of the virtual multi-fracture reconstruction problem is its combinatorial pattern matching aspect. Our main emphasis in this work is to show how the MWGM algorithm can efficiently solve this pattern matching problem. It is relevant to mention that segmentation of broken fragments in more complex multi-fracture situations represents an important though independent problem that is beyond the purview of this paper. For the purpose of illustration, we show here the experimental results on a typical multi-fracture CT image sequence with 6 broken fragments and 10 fracture surfaces altogether (please see Fig. 2). After the initial image processing tasks of thresholding, connected component labeling and area-based filtering are performed, six broken fragments are separated (see Figs. 3 and 4). The two fracture surfaces belonging to the terminal fragments are numbered 1 and 10 and the remaining eight fracture surfaces of the non-terminal fragments are numbered from 2 to 9 as shown in Fig. 5.

Table 1 shows the extreme values of the matching score amongst all possible fracture surface pairs. The higher the value, the better is the compatibility for matching. Thus, fracture surfaces 1 and 4 are excellent candidates for registration while it is highly unlikely that fracture surfaces 4 and 9 would be matched together.

Table 2 shows the solution sets obtained from the MWGM algorithm along with the sum of the edge weights for each solution set. We choose $p = 0.1$, which, in this case, results in the termination of the MWGM algorithm after obtaining two orthogonal solution sets based on Eq. (10). As the score of the first solution is much higher than that of the second, we cannot expect more competetive solutions. The solution pattern clearly demonstrates the effectiveness of the designed score matrix in being able to yield the optimal solution.

Note that the number of reconstruction options for this image sequence is known to be 384 (please see Section 5.1). The MWGM algorithm demonstrates that effective reconstruction can be obtained by exploring just two solutions. On a 1.73 GHz Pentium machine, generation of the solution sets (representing various opposable fracture surface pairs as shown in Table 2) takes much

Table 2
The results from the Graph Matching algorithm.

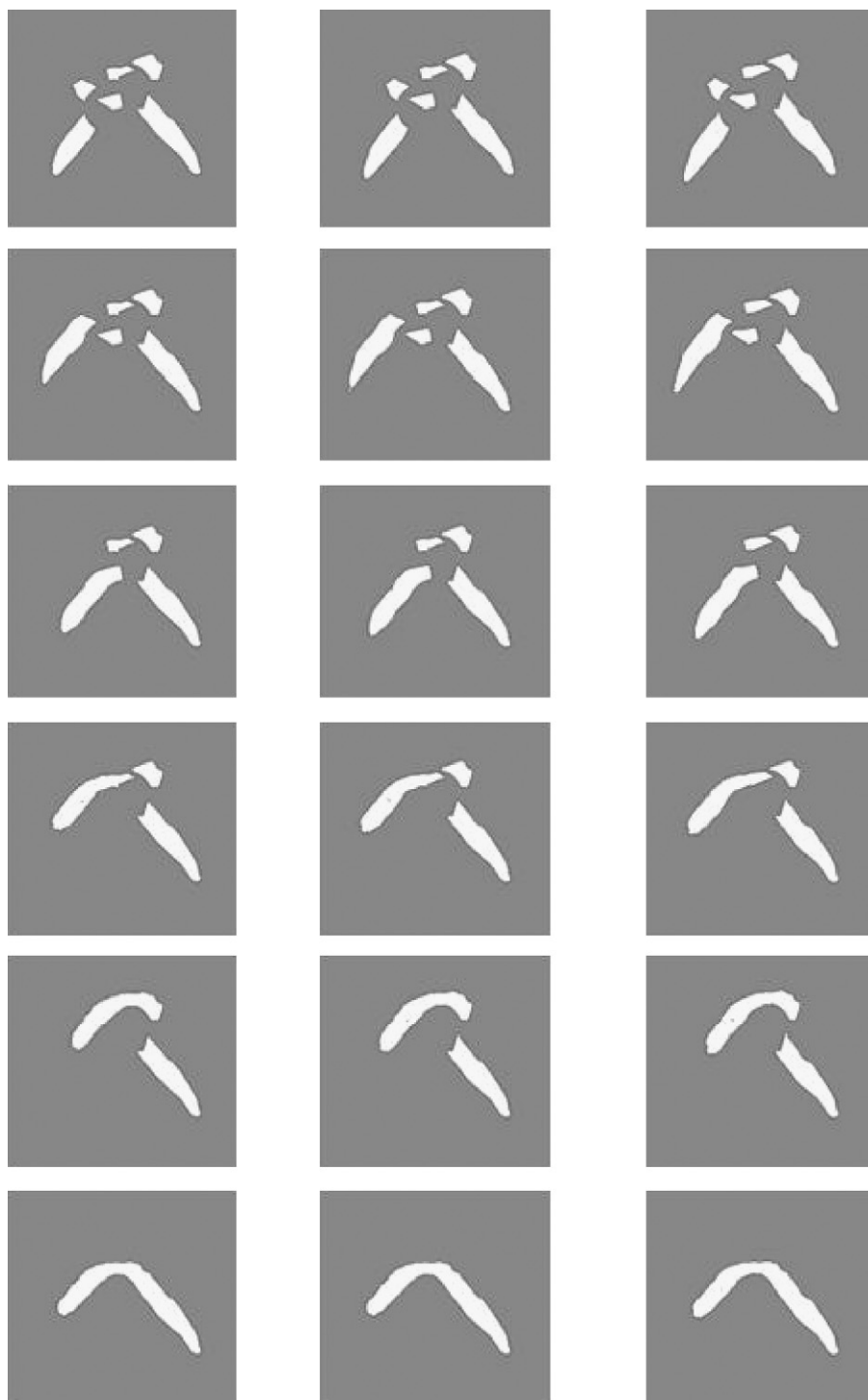| Solution set	Score of the solution set
((1,4), (2, 5), (3, 6), (7, 8), (9, 10))	4987
((1,3), (2, 9), (4, 6), (5, 7), (8, 10))	3123

Fig. 6. Different stages of multi-fracture reconstruction for the three consecutive CT slices shown in Fig. 2.

less than 1 min. Fig. 6 describes the various stages of the reconstruction with the best solution set (obtained from row 1 of Table 2) using the improvised ICP algorithm described in Section 6. The first row shows three successive images in the original CT sequence with six broken fragments or components (denoted by bright intensity values), obtained after preprocessing the original CT image sequence. Each of the later five rows shows the same three images with a new pair of fracture surfaces registered at each stage.

Table 3 describes the results at the end of each step of the procedure for shape monitoring of the partially reconstructed mandible at various stages of reconstruction. At each stage, both shape constraints (defined in Claim 3 in Section 7) are satisfied with a choice of $q = 0.01$ (constraint 2 in Claim 3). Thus, we proceed with the best solution of the MWGM algorithm to complete the registration of all five fracture surface pairs. Rows 2–4 of Table 3 show that the value of $TC_{f,g}$ increases by a relatively small amount when a fragment, which is relatively small in volume, is added to the partially recon-

Table 3
The results of shape monitoring at various stages of the reconstruction process ($A = (2I_g - O_{f,g})/2I_g$).

Various stages of reconstruction	$TC_{f,g}$	A
(1, 4) registered	1.08	0
((1, 4), (2, 5)) registered	1.47	0
((1, 4), (2, 5), (3, 6)) registered	1.57	0
((1,4), (2,5), (3,6), (7, 8)) registered	1.69	0
All 5 fracture surface pairs registered	21.71	0.0003

structed mandible. In the last step of the reconstruction, when a terminal fragment with much larger volume is added to the partially reconstructed mandible by registering the fracture surfaces 9 and 10, the value of $TC_{f,g}$ increases significantly. This is also evident from Fig. 6. The MSE for registration of different pairs of fracture surfaces are within 1–2 mm^2.

9. Conclusions and future directions

We have addressed an important surgical problem of virtual craniofacial reconstruction in the area of biomedical pattern analysis. The problem is appealing from both, an application standpoint and a theoretical perspective. From the application standpoint, we have achieved a fast and accurate reconstruction of a fractured human mandible from several broken fragments, a situation which poses severe challenges for a practicing surgeon. Using our approach, the surgeon can easily identify the opposable fracture surface pairs within a very short period of time. After the identification of the opposable fracture surface pairs, the actual registration of these surfaces can be performed. From a theoretical perspective, on the other hand, the problem clearly resembles a 3D jigsaw puzzle assembly problem which entails significant combinatorial pattern matching. We have employed computer vision and graph matching algorithms to solve this extremely challenging problem. A score matrix is first constructed using a linear combination of inverse Hausdorff distance and a function based on contour curvature. A MWGM algorithm is used next to identify the opposable fracture surface pairs. The individual fracture surface pairs are registered using an MCMW bipartite graph matching algorithm. Finally, the overall reconstruction process is continuously monitored by shape constraints based on computation of the Tanimoto coefficient. The proposed solution has the potential to reduce considerably the operative time, operative cost and patient trauma during actual reconstructive craniofacial surgery.

One direction for future research is to extend the proposed solution for virtual craniofacial reconstruction to other areas of reconstructive surgery involving multiple fractures such as orthopedic surgery. Issues related to the segmentation of bone fragments in CT images exhibiting complex multiple fractures will also be addressed. We also intend to focus on computer vision-guided identification of fracture surfaces and subsequent extraction of fracture surface data to make the proposed virtual reconstruction scheme fully automated.

Acknowledgments

References

[1] King RE, Scianna JM, Petruzzelli GJ. Mandible fracture patterns: a suburban trauma zenter experience. Am J Otolaryngol 2004;25(5):301–7.
[2] Zahl C, Muller D, Felder S, Gerlach KL. Cost of miniplate osteosynthesis for treatment of mandibular fractures: a prospective evaluation. Gesundheitswesen 2003;65(10):561–5.
[3] Bhandarkar SM, Chowdhury AS, Tang Y, Yu JC, Tollner EW. Computer vision guided virtual craniofacial reconstruction. Comput Med Imaging Graph 2007;31(6):418–27.
[4] Chowdhury AS, Bhandarkar SM, Robinson RW, Yu JC. Virtual craniofacial reconstruction from computed tomography image sequences exhibiting multiple fractures. In: Proceedings of the thirteenth IEEE international conference on image processing (ICIP). 2006. p. 1173–6.
[5] Ogundare BO, Bonnick A, Bayley N. Pattern of mandibular fractures in an urban major trauma center. J Oral Maxillofac Surg 2003;61(6):713–8.
[6] Boole JR, Holtel M, Amoroso P, Yore M. 5196 mandible fractures among 4381 active duty army soldiers, 1980 to 1998. Laryngoscope 2001;111(10):1691–6.
[7] Clauser L, Galie M, Mandrioli S, Sarti E. Severe panfacial fracture with facial explosion: integrated and multistaged reconstructive procedures. J Craniofac Surg 2003;14(6):893–8.
[8] Schettler D, Roosen K, Heesen1 J, Kalff R. Timing and techniques of reconstruction and stabilization of combined craniofacial injuries. Neurosurg Rev 1989;12(1):94–105.
[9] Wolfson H, Schonberg E, Kalvin A, Lamdan Y. Solving jigsaw puzzles by computer. Ann Oper Res 1988;12:51–64.
[10] Webster RW, LaFollette PS, Stafford RL. Isthmus critical points for solving jigsaw puzzles in computer vision. IEEE Trans Syst Man Cybern 1991;21(5):1271–8.
[11] da Gama Leitao HC, Stolfi J. A multiscale method for the reassembly of two-dimensional fragmented objects. IEEE Trans Pattern Anal Mach Intell 2002;24(9):1239–51.
[12] Goldberg D, Malon C, Bern M. A global approach to automatic solution of jigsaw puzzles. Comput Geom Theor Appl 2004;28(3):165–74.
[13] Makridis M, Papamarkos N. A new technique for solving a jigsaw puzzle. In: Proceedings of the thirteenth IEEE international conference on image processing (ICIP). 2006. p. 2001–4.
[14] Barequet G, Sharir M. Partial surface and volume matching in three dimensions. IEEE Trans Pattern Anal Mach Intell 1997;19(9):929–48.
[15] Papaionnou G, Karabassi E, Theoharis T. Reconstruction of three-dimensional objects through matching of their parts. IEEE Trans Pattern Anal Mach Intell 2002;24(1):114–24.
[16] Huang QX, Flory S, Gelfand N, Hofer M, Pottmann H. Reassembling fractured objects by geometric matching. ACM Trans Graph 2006;25(3):569–78.
[17] Kampel M, Sablantig R. On 3D mosaicing of rotationally symmetric ceramic fragments. In: Proceedings of the seventeenth IAPR international conference on pattern recognition (ICPR). 2004. p. 265–8.
[18] Willis A, Cooper D. Bayesian assembly of 3D axially symmetric shapes from fragments. In: Proceedings of the sixth IEEE international conference on computer vision pattern recognition (CVPR). 2004. p. 82–9.
[19] Hounsfield GN. Nobel award address. Med Phys 1980;7(4):283–90.
[20] Schwartz JT, Sharir M. Identification of partially obscured objects in two dimensions by matching of noisy characteristic curves. Int J Rob Res 1987;6(2):29–44.
[21] Wolfson H. On curve matching. IEEE Trans Pattern Anal Mach Intell 1990;12(5):483–9.
[22] Huttenlocher DP, Klanderman GA, Rucklidge WJ. Comparing images using the Hausdorff distance. IEEE Trans Pattern Anal Mach Intell 1993;15(9):850–63.
[23] Yarger RWI, Quek FKH. Surface parameterization in volumetric images for feature classification. In: Proceedings of the IEEE international symposium on bio-informatics and biomedical engineering. 2000. p. 297–303.
[24] Costa LF, Cesar Jr RM. Shape analysis and classification, theory and practice. CRC Press; 2000.
[25] Papadimitrou CH, Steiglitz K. Combinatorial optimization—algorithms and complexity. Prentice Hall; 1982.
[26] Christofides N. Graph theory: an algorithmic approach. Academic Press; 1975.
[27] Cormen TH, Leiserson CE, Rivest RL, Stein C. Introduction to algorithms. MIT Press; 2001.
[28] Besl PJ, McKay ND. A method for registration of 3-D shapes. IEEE Trans Pattern Anal Mach Intell 1992;14(2):239–56.
[29] Burdea GC, Wolfson HJ. Solving jigsaw puzzles by a robot. IEEE Trans Rob Autom 1989;5(6):752–64.
[30] Veltkamp RC. Shape matching: similarity measures and algorithms. In: Proceedings of the IEEE international conference on shape modeling & applications. 2001. p. 188–9.
[31] Belongie S, Malik J, Puzicha J. Shape matching and object recognition using shape contexts. IEEE Trans Pattern Anal Mach Intell 2002;24(4), 509:522.
[32] Mills EJ, Dean PM. Three-dimensional hydrogen-bond geometry and probability information from a crystal survey. J Comput-Aided Mol Des 1996;10(6):607–22.

Ananda S. Chowdhury is currently a Reader in the Department of Electronics and Telecommunication Engineering at Jadavpur University, Calcutta, India. From August 2007 to December 2008, he was a postdoctoral fellow in the Department of Radiology and Imaging Sciences at the National Institutes of Health (NIH), Bethesda, MD, USA. He earned his Ph.D. in Computer Science at University of Georgia, Athens, GA, USA in July 2007. Earlier, he received a B.Sc. (with Hons.) in Physics from Presidency College, Calcutta, India in 1996, a B.Tech. in Electronics Engineering from Institute of Radiophysics and Electronics, Calcutta, India in 1999, and an M.E. in Computer Engineering from Jadavpur University, Calcutta, India in 2001. His research interests include computer vision, pattern recognition and image processing. He is a member of the IEEE and IEEE Computer Society.

Suchendra M. Bhandarkar received a B.Tech. in Electrical Engineering from the Indian Institute of Technology, Bombay, India in 1983, and an M.S. and Ph.D. in Computer Engineering from Syracuse University, New York in 1985 and 1989, respectively. He is currently a Professor in the Department of Computer Science at the University of Georgia, Athens, Georgia where he directs the Visual and Parallel Computing Laboratory (VPCL). Dr. Bhandarkar was a Syracuse University Fellow for the academic years 1986–1987 and 1987–1988. He is a member of the IEEE, AAAI, ACM and SPIE. He is a coauthor of the book "Object Recognition from Range Images" (Springer Verlag, 1992). He is also a member of the honor societies Phi Kappa Phi and Phi Beta Delta. His research interests include computer vision, pattern recognition, multimedia systems, artificial intelligence and parallel algorithms and architectures for computer vision and multimedia. He has over 100 published research articles in these areas including over 50 articles in peer-reviewed archival journals. Dr. Bhandarkar serves on the editorial boards of the Computer Journal, Applied Intelligence Journal and the Machine Vision and Applications Journal and on the program committees of several international conferences and symposia. He serves as a consultant to government agencies such as NASA, Department of Defense, Department of Energy and Department of Health and Human Services.

Robert W. Robinson is a Professor in the Department of Computer Science at the University of Georgia, Athens, GA, USA. He earned his Ph.D. at Cornell in Mathematics in 1966. After a postdoctoral year at the Institute for Advanced Studies in Princeton under the aegis of Kurt Gödel he has held academic appointments at U.C. Berkeley, U. of Michigan, Newcastle U. (Australia), and Southern Illinois U. In 1984 he moved to UGA and served as Head of the Computer Science Department until 1993.

Jack C. Yu is a Professor and Chief of Plastic Surgery and Chief of Pediatric Plastic Surgery as well as the Director of the MCG Craniofacial Center at the MCG Children's Medical Center and currently heads the monthly Cleft Lip and Palate and the Craniofacial programs at MCG. He completed medical school at the University of Pennsylvania. He completed his residency in general surgery and plastic surgery at the Hospital of the University of Pennsylvania. Dr. Yu also completed his craniofacial surgery fellowship at the Hospital of the University of Pennsylvania and Children's Hospital of Philadelphia. Dr. Yu is board certified by the National Board of Dental Examiner, Northeast Regional Board in Dentistry, American Board of Surgery and the American Board of Plastic Surgery. He is currently on the Biomaterials and Research Committee for the American Society of Maxillofacial Surgeons, Member of the Advisory Council for Mathematical Sciences for the State of Georgia, Continuing Education Committee for the American Cleft Palate-Craniofacial Association, and Development Committee for the Plastic Surgery Research Council, and International Society of Craniofacial Surgeons. His clinical interests focus on deformities of the craniofacial region in both adults and children, as well as cosmetic surgeries of the face.